Industrial Crops & Products 243 (2026) 123076

Contents lists available at ScienceDirect

Industrial Crops & Products

journal homepage: www.elsevier.com/locate/indcrop

Effect of sub-zero temperature, moisture content and loading rate on the bending strength of beech and birch wooden dowels

Angelo Aloisio [a], Yue Wang [b,d,*], Matteo Pelliciari [c], Yue Liu [b], Massimo Fragiacomo [a]

[a] Department of Civil Construction-Architecture and Environmental Engineering, University of L'Aquila, Italy
[b] Research Institute of Urbanization and Urban Safety, School of Future Cities, University of Science and Technology Beijing, 30 Xueyuan Road, Beijing 100083, China
[c] DIEF, Department of Engineering "Enzo Ferrari", via P. Vivarelli 10, 41125 Modena, Italy
[d] Department of Civil and Architectural Engineering, The Royal Institute of Technology, Stockholm, Sweden

ARTICLE INFO

Keywords:
Wooden dowels
Sub-zero temperature
Scanning electron microscope
Sustainable timber construction
Nonlinear analysis

ABSTRACT

Wooden dowels are emerging as a promising alternative or complement to adhesives in adhesive-free timber products and pure-wood structural joints. The performance of these connections is critically governed by the mechanical properties of the dowels, which can be influenced by environmental and loading conditions. This study experimentally evaluated the bending strength of approximately 100 beech and birch dowels (diameter 16 mm) under two temperatures (20 °C and −20 °C), two moisture states (dry and water-soaked), and five loading rates (0.04 to 25 mm/min). Four-point bending tests were conducted in accordance with EN 408 using a constant-rate displacement protocol, and moisture content was determined gravimetrically for each conditioning state. The results were statistically assessed using a linear mixed-effects (LME) model to quantify main effects and interactions among species, temperature, moisture state, and loading rate. Birch dowels consistently outperformed beech, with an average strength margin of 19%. Moisture content emerged as the dominant factor, with soaking causing a mean 47% strength reduction, while cooling to −20 °C provided only modest gains (5%–8%), particularly in wet specimens. Rate sensitivity was notable in dry dowels but became negligible once saturated. An empirical design model was proposed to estimate a modification factor for predicting bending strength, incorporating temperature–moisture interactions and rate effects, and calibrated for 95% reliability. SEM (Scanning Electron Microscopy) observations indicated that moisture promotes more ductile fracture through fibre pull-out, whereas freezing partially restores matrix stiffness, resulting in cleaner and more brittle fracture surfaces. The results provide practical modification factors for dowel design under coupled environmental and rate effects, supporting more robust and sustainable dowel-based connection systems. Future work should extend the experimental matrix to intermediate temperatures and moisture levels and assess long-term and cyclic actions (e.g., fatigue and freeze–thaw exposure) to further support standardization and code implementation.

1. Introduction

The mechanical properties of wood are affected by the scale effect (Golovin et al., 2022), largely due to the occurrence of defects (Beall, 2000), which distinguishes clear wood from structural timber containing natural or processing-induced irregularities (Kretschmann, 2010). This distinction is central to defining design values, calibrating safety factors, and ensuring reliability under service and extreme loading. While temperature, moisture content, deformation rate, and treatment effects have been widely investigated using small, homogeneous clear-wood specimens for experimental convenience, only limited recent work has addressed these sensitivities in full-scale members. In this regard, laminated timber studies are particularly relevant because they capture interactions among wood microstructure, adhesive interfaces, and defects, highlighting that full-scale behaviour involves additional complexities that are not represented in small-scale tests.

Despite progress, further research is needed on the long-term effects of loading scenarios such as impact and fatigue, particularly for timber structures in cold and humid climates where seasonal fluctuations may affect connection performance over time.

In parallel, the use of wooden dowels is growing, mainly (i) as an alternative to adhesives in adhesive-free laminated wood products and

* Corresponding author.
E-mail address: yue4@kth.se (Y. Wang).

https://doi.org/10.1016/j.indcrop.2026.123076
Received 30 September 2025; Received in revised form 7 March 2026; Accepted 11 March 2026
Available online 16 March 2026

(ii) as pegs in structural joints. Since mass timber construction still relies predominantly on metal fasteners, wooden dowels represent a promising biobased alternative to both metal fasteners and chemical adhesives (Sotayo et al., 2020; Han et al., 2023; Branco and Descamps, 2015; Aloisio et al., 2025a,b; Wang et al., 2025; Tomasi et al., 2025; Derikvand and Khoshroodi, 2025; Wang et al., 2026), offering improved compatibility with timber substrates (reversible assembly and recyclability), reduced dependence on synthetic adhesives, and potential benefits in fire performance, weight, and aesthetics.

Dowel-type timber joints have been extensively studied with respect to failure modes (Frontini et al., 2020; Pranata et al., 2021), shear capacity under different mechanisms (Miller et al., 2010), and factors controlling shear strength (Jung et al., 2008; Bohan et al., 2022), showing that dowel material properties, diameter, and processing significantly influence joint capacity. Moreover, connection systems using wooden dowels and corresponding capacity models have also been investigated (Vilguts et al., 2024; De Santis et al., 2025). However, the mechanical behaviour of the dowel itself remains critical: as first noted by MacKay (1997), a common dowel failure mode results from combined bending and shear (Mode V) (MacKay, 1997; Miller et al., 2010; Aloisio et al., 2026), which is distinct from simple cross-grain shear failure or plastic-hinge formation (Miller et al., 2010). Although many experimental studies on single- and double-shear joints are available (Sandberg et al., 2000; Xu et al., 2022; Judd et al., 2012; Milch et al., 2017; Riggio et al., 2016; Teodorescu et al., 2020; Ceraldi et al., 2008, 2012, 2018; Grönquist et al., 2019), they rarely isolate or quantify the coupled effects of temperature, moisture content, and loading rate on the dowel element itself, despite their direct implications for connection capacity.

Given the increasing interest in sustainable and bio-based construction materials (Haftkhani et al., 2022), further research on wooden dowels under varying environmental and loading conditions is needed to improve the robustness of dowel-based connection systems. Owing to their geometry and service conditions, wooden dowels cannot be fully equated to clear wood, motivating dedicated experimental studies to clarify their macro- and micro-scale behaviour and support future standardization. In this context, the present study investigates the bending strength of beech wood dowels at sub-zero temperature, under different moisture states and loading rates, with the aim of informing reliable modification factors and design provisions for codes and practice.

The performance of connections using wooden dowels depends directly on the dowels' bending and shear strength, which are key inputs in Eurocode-type capacity models and those proposed by Miller (2004). Therefore, quantifying the influence of temperature, moisture content, and loading rate on dowel bending strength is essential for an accurate assessment of connection capacity.

In timber joints employing hardwood dowels, the loading rate can vary from quasi-static service conditions to transient or accidental actions, and rate-dependent dowel strength may therefore influence both capacity and failure mode, particularly under non-ambient temperature and moisture conditions. The contribution this study aims to make, in terms of innovation and originality, can be summarized as follows: (i) Experimental estimation of the bending strength of beech and birch wooden dowels used in pure-wood timber joints or adhesive-free timber panels, considering the effects of deformation rate, moisture content, and sub-zero temperature. (ii) Statistical evaluation of the significance of these parameters on the bending strength, ensuring robust data analysis. (iii) Microstructural analysis using SEM to assess the impact of temperature and moisture content on the fracture surface of the dowels. (iv) Development of an empirical model for estimating the modification factor to predict the bending strength of wooden dowels.

2. Experimental tests

The experimental activities, detailed in the following subsections, follow the workflow shown in Fig. 1.

Table 1
Geometric and material properties of the Birch and Beech wooden dowels used in this study.

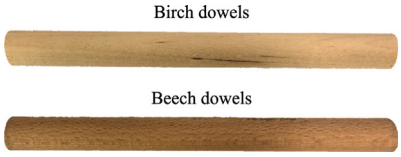

Material	Diameter [mm]	Length [mm]	Wood density	
			Mean [kg/m^3]	CoV [%]
Beech	16	185	755.8	6.2
Birch	16	185	668.3	3.5

2.1. Wooden dowels

The wooden dowels analysed in this study were manufactured from two hardwood species: beech (*Fagus sylvatica L.*) and birch (*Betula pendula Roth*). Both dowel types share the same nominal geometry, with a diameter of 16 mm and a length of 185 mm (both are nominal values).

The beech dowels provided by BIOHABITAT srl in Italy are routinely used in adhesive-free cross-laminated timber (CLT) systems, where they are inserted in a staggered layout to mechanically interlock the orthogonal timber layers. The birch dowels were provided by Björkträ Timber AB (Arbrå, Sweden) and were rotary cut products from knot-free sideboards to minimize imperfections. The geometric and physical properties of the two dowel types are summarized in Table 1.

Although identical in size, the two species show marked differences in density. Beech dowels exhibit a higher mean density (755.8 kg/m^3) compared to birch (668.3 kg/m^3). Additionally, birch dowels demonstrate a more consistent material quality, with a lower coefficient of variation (3.5%) as compared to beech (6.2%).

Specifically, to capture moisture-dependent behaviour, experiments were conducted at two target moisture content levels, which are herein denoted as 'dry' and 'wet' conditions. In this paper, the term dry is used for brevity to indicate the air-dry conditioning state (20 °C and 65% RH).

'Dry' wooden dowels were conditioned at the indoor climate of 20 °C and 65% relative humidity levels for at least three weeks prior to the experiment taking place, while 'Wet' wooden dowels were first dry conditioned for three weeks and then water-soaked (temperature: 20 °C) for at least two more days.

Moreover, the varying moisture content levels among the 'dry' and 'wet' dowels were also combined with two different temperature settings: ambient (20 °C) and sub-zero (−20 °C), allowing for the assessment of low-temperature embrittlement effects (as illustrated in Fig. 2)a. Specifically, half of the 'dry' and 'wet' dowels, after being conditioned as per the respective requirements, were additionally frozen inside a climate chamber with sub-zero temperature (−20 °C) for at least two extra days before the experiment took place (as shown in Fig. 2b).

However, it is worth mentioning that the water-soaking took place before the freezing stage of the wooden dowels, as the sub-zero climate is inherently dry, which can contribute to a decrease in moisture content for both 'Dry' and 'Wet' specimens. This issue will be presented in more depth in Section 3.1.

2.2. Experimental procedure

Table 2 presents the test matrix used in the experimental campaign, which was designed to systematically investigate the effects of loading rate, moisture content, and temperature on the bending strength of dowels made of beech and birch. Loading rates were selected to span quasi-static bound (0.04–0.2 mm/min), standard laboratory practice

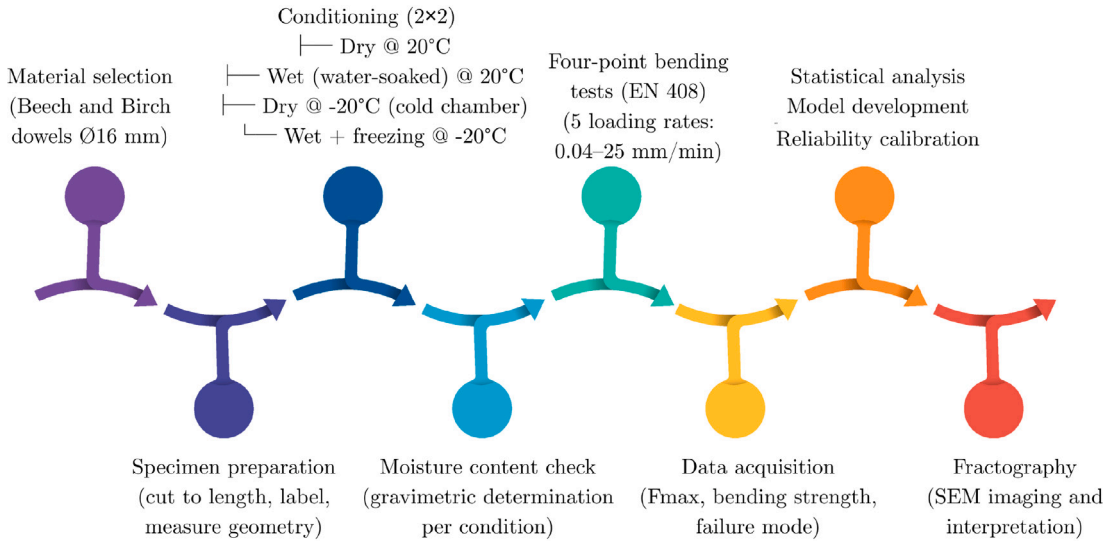

Fig. 1. Workflow of the research methodology adopted in this study.

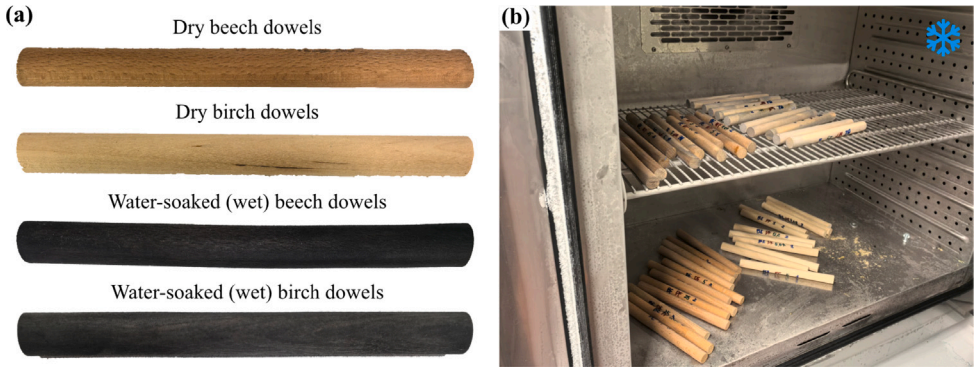

Fig. 2. (a) Representative wooden dowel configurations, (b) wooden dowels conditioned under sub-zero temperature in a climate chamber.

Table 2
Test matrix, reporting the test repetitions for different values of load rate, moisture content, and temperature.

	Load rate [mm/min]					Conditioned Climate	Temperature [° C]
	25	5	1	0.2	0.04		
Test rep.	3	3	3	3	2	Dry	20
	3	3	3	3	2	Wet (Water soaked)	
	3	3	3	3	2	Dry	−20
	3	3	3	3	2	Wet (Water soaked)	

(1–5 mm/min), and an upper quasi-static bound (25 mm/min) to probe logarithmic rate trends.

Each combination of conditions was replicated to ensure statistical robustness. The number of specimens per configuration was generally three per loading rate, with two replicates at the lowest rate (0.04 mm/min), due to extended test durations.

Given the varying moisture contents, temperature, and loading rates, four different so-called climate categories can be distinguished:

- 'D': The dowels were conditioned under dry climates (20 °C; 65% RH) and tested right after conditioning.
- 'W': The dowels were water-soaked (20 °C) and tested right after conditioning.
- 'DF': The dowels were first conditioned under dry climates (20 °C; 65% RH) and then frozen at sub-zero temperatures (−20 °C) before being tested.
- 'WF': The dowels were water-soaked (20 °C) and then frozen at sub-zero temperatures (−20 °C) before being tested.

The authors acknowledge that only two temperature levels and two moisture states were considered; therefore, the observed trends should be interpreted within the investigated ranges, and additional intermediate conditions and broader climatic scenarios are recommended for future work to fully characterize environmental sensitivity.

As for notations, the specimens are denoted in the form of:

'Species'_'Conditions'_'Loading rate'_Replicate

where Species are either 'BI' (for birch) or 'BE' (for beech); Conditions are either 'D' (for dry) or 'W' (for wet) or 'DF' (for dry dowels frozen under sub-zero climates) or 'WF' (for wet dowels frozen under sub-zero climates); Loading rate are either '0.04' or '0.2' or '1' or '5' or '25' mm/min. For example, the notation 'BI_DF_25' indicates a birch dowel conditioned first under dry and then under sub-zero climates and tested under the loading rate of 25 mm/min.

During testing, temperature and moisture conditions were kept effectively constant by (i) conditioning the dowels to the target state

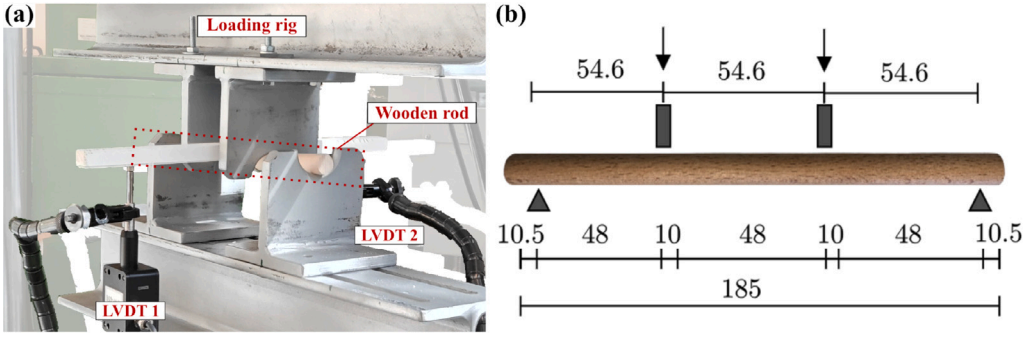

Fig. 3. (a) View of the experimental setup for the bending tests, (b) test setup with all dimensions (unit: mm).

prior to testing and (ii) testing the sub-zero specimens immediately after removal from the cold chamber. In practice, the thermal inertia of the specimens and the absence of liquid water exposure during the test mean that neither temperature nor moisture content can change appreciably over the few minutes required to reach failure.

For the setup, four-point bending tests were conducted to evaluate the bending properties of the dowels, aiming to rule out the effect of shear force. The tests have been performed according to EN 408 (EN-408, 2003). All tests were performed on an MTS 810 with a capacity of 100 kN, with the load signals collected by a built-in load cell. Two LVDTs were fixed onto the test machine's bottom platen via two magnetic bases. An angle cantilever is fixed on the middle portion of the wooden dowels, the mid-span deflection of which was captured via the probes of two LVDTs (see Fig. 3). The maximum value of the force–displacement curves led to the assessment of the bending moment in the central portion of the dowel at failure (M_u) and the shear in the lateral portion of the dowel at failure (T_u). The bending strength has been assumed as the bending stress at the outermost dowel fibres at dowel failure and calculated with the Navier formula:

$$f_m = \frac{M_u}{I}\frac{d}{2} \tag{1}$$

where M_u is the bending moment in the central portion of the dowel at failure, d is the dowel diameter, and I is the second moment of area of the dowel.

2.3. Statistical analysis

A linear mixed-effects (LME) model (Pinheiro and Bates, 2000) was fitted to the complete data set to account simultaneously for fixed experimental factors and the hierarchical replicate structure of the tests. Bending strength (f_m) was the response, while wood species (Beech, Birch), moisture content from Table 3, temperature (20 °C, −20 °C) and the base-10 logarithm of loading rate [$\log_{10}(v)$, mm min^{-1}] were entered as fixed effects, including all interaction terms up to fourth order. A specimen identifier was entered as a random intercept, which captures the correlation between the three repeats within each configuration and avoids inflating the residual variance (West et al., 2015).

Model residuals were examined via a normal Q–Q plot and a residual-versus-fitted scatter plot (Field and Miles, 2012). Fixed-effect significance was assessed with Type-III marginal F-tests using Satterthwaite denominator degrees of freedom (Satterthwaite, 1946; Luke, 2017). The resulting ANOVA is given in Table 7; in the column "*F(1102)*" the subscripts $df_1 = 1$ and $df_2 = 102$ denote, respectively, the numerator and Satterthwaite-adjusted denominator degrees of freedom common to all contrasts. This Type-III/Satterthwaite combination yields order-independent tests and controls the liberal bias that Type-I sums-of-squares can introduce in unbalanced designs (Kuznetsova et al., 2017).

3. Results

The results are presented in four subsections: (1) analysis of the force–displacement curves, (2) descriptive statistics of the bending strength and (3) statistical tests to assess the significance of differences among groups, considering the combined influence of the three parameters: temperature (20 °C and −20 °C), moisture content, and loading rate (0.04, 0.2, 1, 5, and 25 mm/min).

3.1. Force–displacement curves and failure modes

Fig. 4 shows the force–displacement curves for beech dowels, while Fig. 5 presents the results for birch dowels. A clear difference is observed between the two wood species, with birch outperforming beech in terms of higher load-carrying capacity and reduced variability in mechanical response.

Apart from these differences, the trends within each wood species appear consistent. The highest strength is generally observed in dry conditions at both −20 °C and 20 °C, with only minor differences between the two, slightly higher at −20 °C, though moderately so. Moisture content significantly impairs performance, not only reducing peak strength but also altering the overall response.

The worst condition occurs at 20 °C under high moisture content, while a slightly improved, yet still limited, response is observed at −20 °C. The performance difference between −20 and 20 °C is more evident in wet conditions than in dry ones. As expected, increased moisture content leads to a more ductile response due to water-induced plasticization; this ductility persists at sub-zero temperature, although it is moderately reduced at −20 °C.

Typical failure modes of birch and beech dowels under various climate conditions are presented in Fig. 6. The path of crack initiation and propagation was marked with red lines. It is worth noting that not all specimens at different loading rates are presented, as their failure modes are visually alike. The microstructure of the fracture surfaces of the dowel specimens can be better visualized using scanning electron microscopy (SEM) techniques, the details of which will be presented in Section 5.

Discussions on the moisture contents shall be supplemented, and the MC levels for beech and birch dowels, conditioned under all various climates, are presented in Table 3. It is evident that Beech and Birch dowels yielded similar trends, with only slight differences in means and standard deviations. As a result of the influence of climate conditions, it is noticeable that the Moisture content reaches the lowest under Dry/−20 °C for both species (MC ≈ 10%–11%). Under Wet/20 °C conditions, the MC reaches its highest for both species (≈ 67%).

It is noticeable that when the temperature lowers from 20 °C to −20 °C, the MC generally reduces, especially in wet conditions (e.g., Beech: from 67.24% to 24.40%, Birch: from 67.60% to 23.83%). As mentioned before in Section 2, the dowels were water-soaked before being frozen. Since the sub-zero climate was inherently dry, the freezing process contributed to a decrease in moisture content for both 'Dry' and 'Wet' specimens.

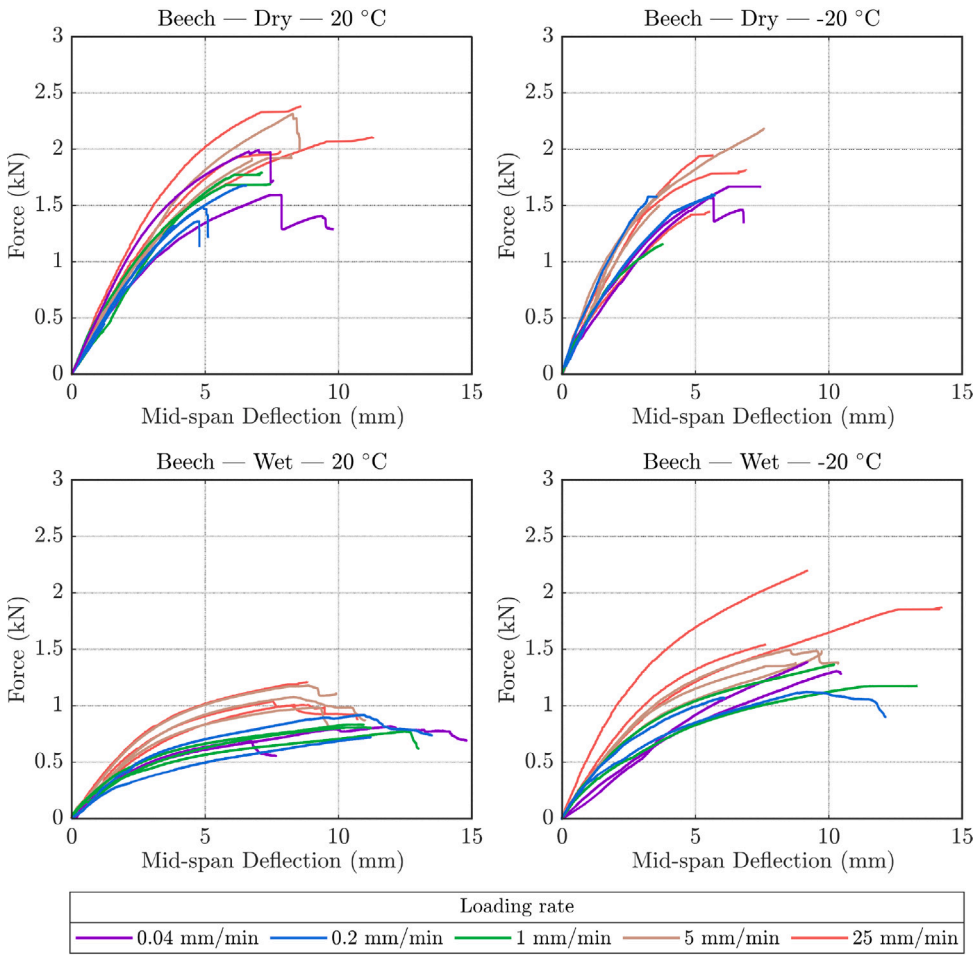

Fig. 4. Force–displacement curves from 4-point bending tests on beech specimens under different environmental and loading conditions. Each subplot represents a combination of temperature (20 °C or −20 °C) and moisture content (dry or wet). Curves are colour-coded by loading rate: 0.04, 0.2, 1, 5, and 25 mm/min.

Table 3
Moisture contents for beech and birch dowels conditioned at various conditions.

Dowels types & Conditions		Dry/20 °C	Wet/20 °C	Dry/ −20 °C	Wet/ −20 °C
Beech	Mean	11.20%	67.24%	10.00%	24.40%
	Std	0.4%	3.5%	1.0%	1.5%
Birch	Mean	11.30%	67.60%	11.00%	23.83%
	Std	0.6%	3.0%	1.7%	3.7%

3.2. Descriptive statistics

Fig. 7 offers a visual comparison of bending-strength distributions for all environmental conditions. In every quartet of boxes, the light–brown birch boxes sit systematically above the lighter beech ones. The impact of moisture is even more evident: both species lose roughly half their strength when soaked, and the change in scale is evident in the compressed wet boxes. Cooling to −20 °C raises the median in every dry group but leaves the dry groups essentially unchanged. Finally, the whisker lengths show that relative scatter (CoV) is smallest for Birch–Dry −20 °C and highest for the two wet Beech conditions, suggesting that wetting not only weakens the dowels but also increases variability.

Table 4 translates Fig. 7 into numbers. The mean strength of dry Birch at −20 °C reaches 135 MPa, whereas wet Beech at 20 °C averages only 49 MPa, a reduction of about 64%. CoV confirms the box-plot whiskers: dry Birch shows the tightest distribution (CoV = 0.12), while wet Beech at −20 °C exhibits the largest relative spread (CoV = 0.23).

In summary, the tests reveal three consistent trends:

- Species effect: Birch outperforms Beech by 13–23 MPa.
- Moisture effect: Wetting reduces strength by 45–55 MPa regardless of species or temperature.
- Temperature effect: Cooling benefits mainly wet specimens, lifting the median by 7–25 MPa.

Fig. 7 and Table 4 show that material choice and moisture control dominate mechanical performance, while low-temperature operation offers a secondary advantage limited to dry dowels.

Why Birch outperforms the nominally denser Beech can be traced to its anatomy rather than bulk density. Beech is diffuse-porous with large early-wood vessels that interrupt the fibre continuum and act as stress concentrators, whereas Birch vessels are smaller and more evenly distributed, providing a more homogeneous load path (Panshin and de Zeeuw, 1980; Wagenführ, 2006). Beech also contains a larger volume fraction of thin rays (> 16 %), creating weak radial planes susceptible to crack deflection, while Birch rays are fewer and thicker, enhancing toughness (Laboratory, 2010). Moreover, Birch fibres exhibit a lower microfibril angle and higher cellulose crystallinity, both of which translate into higher tensile cell-wall strength despite a ≈12% lower density (Cave, 1968; Donaldson, 2008).

Fig. 8 shows how bending strength responds to changes in loading rate (v = 0.04–25 mm min^{-1}) once moisture and temperature are fixed. For dry specimens (top row) both species exhibit an apparent, approximately logarithmic rate sensitivity: moving from the quasi-static regime (0.04–0.2 mm min^{-1}) to the impact-like regime (25 mm min^{-1}) increases the mean strength by about 30–35 MPa for Birch and 20–25 MPa for Beech. The gain is slightly larger at −20 °C, in

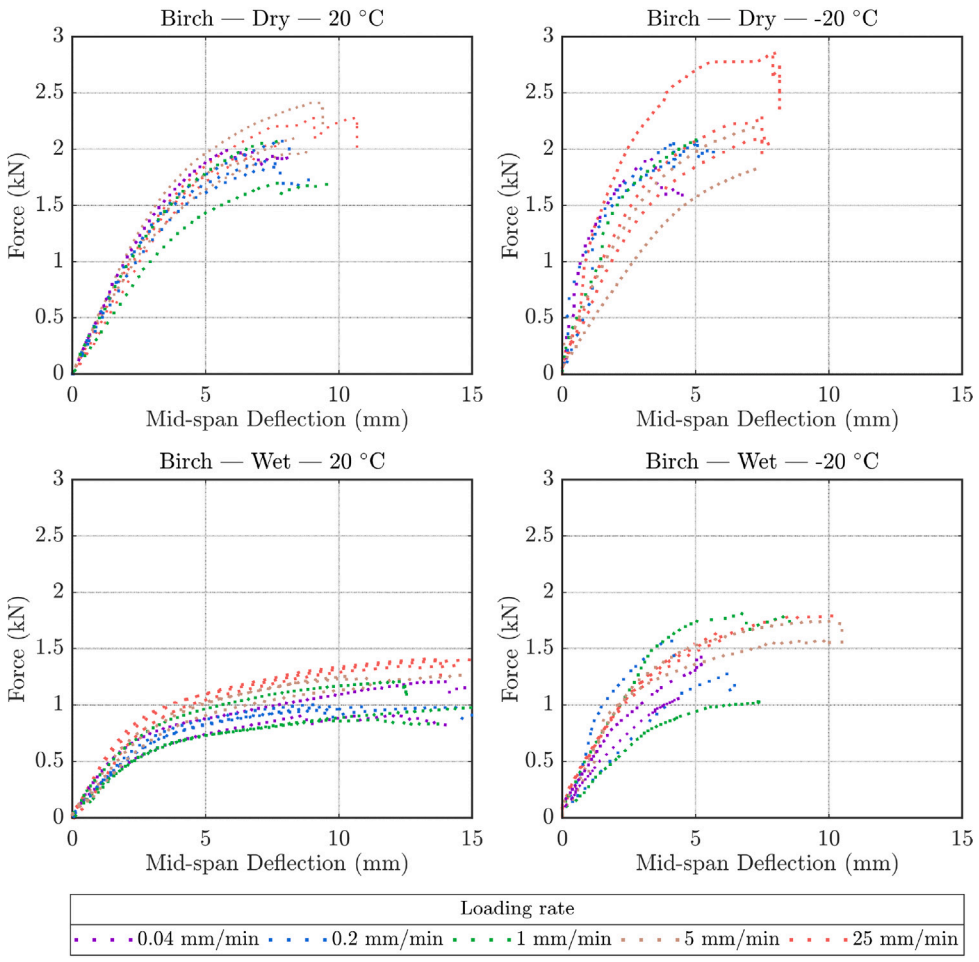

Fig. 5. Force–displacement curves from 4-point bending tests on birch specimens under different environmental and loading conditions. Each subplot represents a combination of temperature (20 °C or −20 °C) and moisture content (dry or wet). Curves are colour-coded by loading rate: 0.04, 0.2, 1, 5, and 25 mm/min.

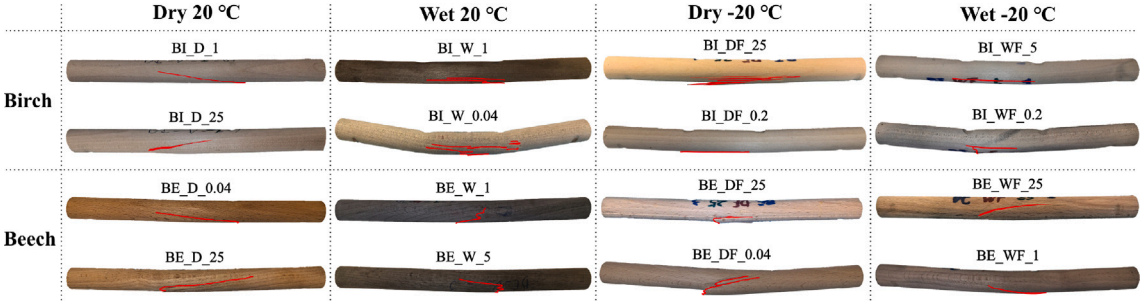

Fig. 6. Typical failure modes of wooden dowels conditioned at varying moisture contents and climates, tested at different loading rates.

Table 4
Descriptive statistics of bending strength (f_m) grouped by wood species, moisture content, and temperature. Mean = arithmetic mean of f_m; Median = 50th percentile; Q1 = 25th percentile (first quartile); Q3 = 75th percentile (third quartile); Min and Max = minimum and maximum observed values; Std = standard deviation; CoV = coefficient of variation, calculated as Std / Mean. Statistics are computed across all loading rates for each combination.

Group	Num of replicates	Mean (MPa)	Median (MPa)	Q1 (MPa)	Q3 (MPa)	Min (MPa)	Max (MPa)	Std (MPa)	CoV
Beech | Dry | −20 °C	12	111.2	104.9	99.6	124.1	74.2	155.8	21.0	0.2
Beech | Dry | 20 °C	14	119.5	121.3	107.3	128.5	87.4	153.6	19.1	0.2
Beech | Wet | −20 °C	12	82.5	79.6	69.3	87.1	60.2	131.1	19.4	0.2
Beech | Wet | 20 °C	14	48.9	49.6	42.2	54.3	36.8	62.8	8.0	0.2
Birch | Dry | −20 °C	11	134.5	130.8	124.8	135.9	118.8	178.2	16.6	0.1
Birch | Dry | 20 °C	14	124.1	126.7	120.6	132.1	79.6	147.7	17.1	0.1
Birch | Wet | −20 °C	11	83.7	92.6	73.1	93.6	59.3	99.4	14.5	0.2
Birch | Wet | 20 °C	14	61.0	61.8	52.3	68.4	47.1	76.1	9.9	0.2

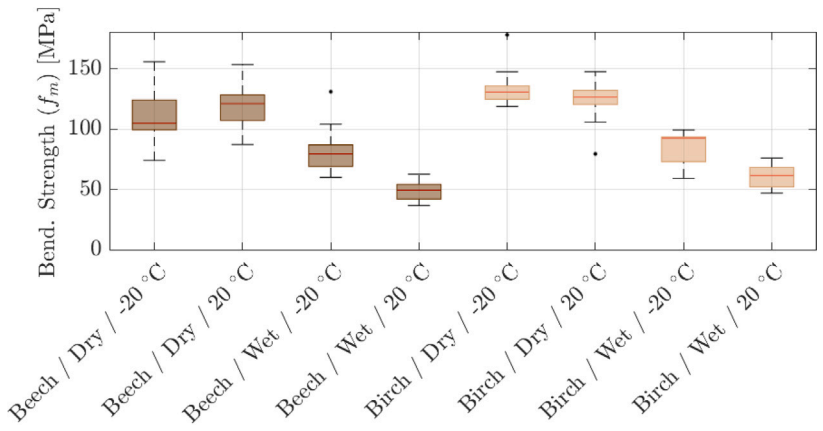

Fig. 7. Boxplots of bending strength (f_m) for Beech and Birch under different environmental conditions (dry/wet, −20 °C/20 °C). Each box displays the interquartile range (IQR), the median (represented by the horizontal line), and whiskers extending to 1.5 times the IQR. The dots represent the outliers.

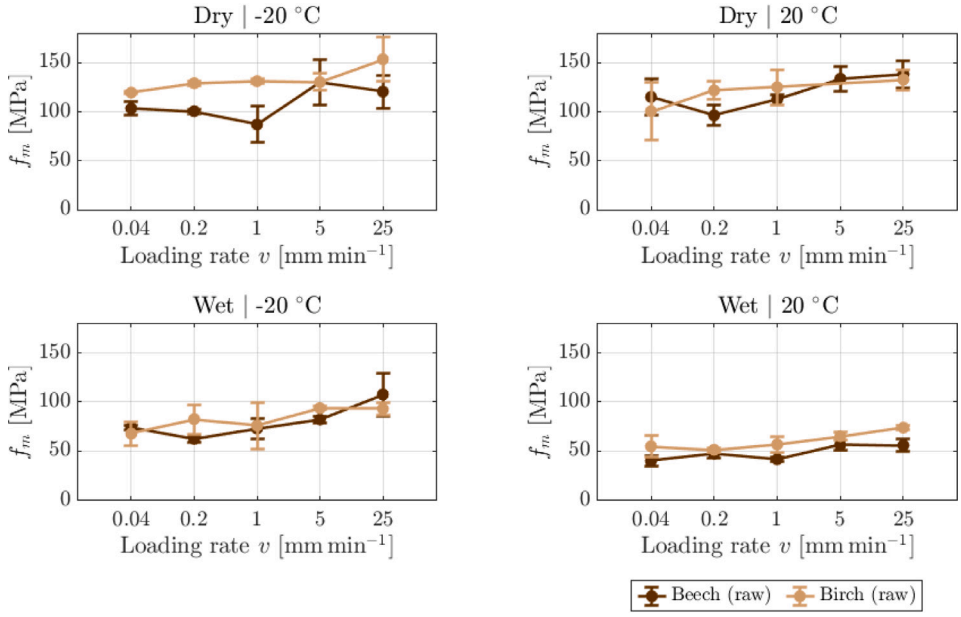

Fig. 8. Effect of loading rate on bending strength (f_m) for Beech and Birch under different environmental conditions. Each subplot shows mean values with standard deviations across loading rates (0.04–25 mm/min) for combinations of moisture content (dry/wet) and temperature (−20 °C/20 °C).

line with the significant Temperature × MC interaction later identified in the mixed-effects ANOVA. In wet specimens (bottom row), the rate effect vanishes: each curve is nearly horizontal and the average slope over three decades of v is below 5 MPa. This attenuation confirms that water plasticizes the cell-wall matrix and suppresses rate-dependent stiffening. Across all four panels, Birch remains consistently stronger than Beech, yet the Species × $\log_{10}(v)$ interaction is non-significant ($p = 0.87$), indicating that both species share the same rate sensitivity when moisture and temperature are held constant. Therefore, it is manifest that the loading rate is a secondary but non-negligible design variable for dry dowels, but its influence disappears once the wood is saturated.

Tables 5 and 6 list the mean ($\overline{f_m}$) and standard deviation (σ_{f_m}) of bending strength measured at five loading rates for birch and beech, respectively.

It is confirmed that, for both species, the rate sensitivity is monotonic and approximately logarithmic, but the magnitude of this sensitivity differs. Birch–Dry shows the most relevant gain: at 20 °C the mean rises from 101 MPa (0.04 mm min^{-1}) to 133 MPa (25 mm min^{-1}), an increase of +32 MPa or ∼ 32%. Under the colder setting (−20 °C), the gain is comparable in absolute terms (+34 MPa) but starts from a higher baseline, leading to a slightly smaller relative change (+28%). Beech–Dry follows the same trend yet with a milder slope: +25 MPa at −20 °C and +23 MPa at 20 °C, i.e. a 20–22% improvement.

Once the specimens are saturated, the rate effect is markedly attenuated. For Birch, the mean strength fluctuates within a narrow band (roughly 68–94 MPa at −20 °C and 51–74 MPa at 20 °C) and the net change from slow to fast loading never exceeds 20 MPa. Beech behaves similarly, with gains of 15–25 MPa that barely compensate for the ≈ 55 MPa penalty from wetting. Cooling from 20 °C to −20 °C amplifies the rate effect in the dry state (slightly higher slopes) but has little influence once the wood is wet. In practical terms, controlling moisture or switching species is more effective than adjusting the loading rate for wet connections.

3.3. Statistical analysis

Table 7 displays the ANOVA results from the linear mixed-effects (LME) model for bending strength.

It can be observed that wood species is highly significant ($p = 6.7 \times 10^{-6}$), with Birch exceeding Beech by roughly 22 MPa. MC has the largest single impact ($F = 35.6$), effectively halving strength

Table 5
Mean and standard deviation of bending strength (f_m) for each test configuration of beech dowels. The factors considered are: wood Species (Beech, Birch), Moisture condition (Dry, Wet), Temperature (−20 °C or 20 °C), and loading Speed in mm/min. For each combination, the number of specimens tested (No. Samples), the arithmetic mean (Mean), and standard deviation (Std) of f_m are reported.

Species	Moisture	Temperature	Speed [mm/min]	No. Samples	Bend. Strength [MPa]	
					Mean	Std
Beech	Dry	−20 °C	0.04	2	103.29	6.55
			0.2	2	100.55	1.98
			1	2	87.07	18.27
			5	3	130.19	22.73
			25	3	120.56	16.66
		20 °C	0.04	2	115.10	18.40
			0.2	3	96.34	10.08
			1	3	112.60	5.26
			5	3	133.68	12.75
			25	3	138.20	13.51
	Wet	−20 °C	0.04	2	74.36	2.48
			0.2	2	62.52	3.29
			1	2	73.01	10.06
			5	3	82.30	3.63
			25	3	107.75	21.80
		20 °C	0.04	2	40.11	4.67
			0.2	3	47.19	4.56
			1	3	41.85	2.00
			5	3	56.39	4.83
			25	3	56.00	6.10

Table 6
Mean and standard deviation of bending strength (f_m) for each test configuration. The factors considered are: wood Species (Beech, Birch), Moisture condition (Dry, Wet), Temperature (−20 °C or 20 °C), and loading Speed in mm/min. For each combination, the number of specimens tested (No. Samples), the arithmetic mean (Mean), and standard deviation (Std) of f_m are reported.

Species	Moisture	Temperature	Speed [mm/min]	No. Samples	Bend. Strength [MPa]	
					Mean	Std
Birch	Dry	−20 °C	0.04	2	119.52	0.99
			0.2	2	129.03	2.45
			1	2	131.10	2.02
			5	2	130.18	8.83
			25	3	153.39	22.49
		20 °C	0.04	2	100.61	29.74
			0.2	3	121.73	9.11
			1	3	124.98	17.47
			5	3	130.10	11.45
			25	3	135.34	11.08
	Wet	−20 °C	0.04	2	67.87	11.72
			0.2	2	82.64	14.98
			1	2	75.99	23.55
			5	2	93.91	1.80
			25	3	93.10	6.65
		20 °C	0.04	2	55.02	11.14
			0.2	3	51.47	2.36
			1	3	56.91	8.33
			5	3	65.31	4.12
			25	3	73.91	2.11

Table 7
Type-III ANOVA (linear mixed-effects) for bending strength f_m. Fixed effects: wood species, moisture content (MC), temperature, and $\log_{10}$ loading rate, including all two- and three-way interactions. The column $F(1102)$ reports the F-statistic with numerator df = 1 and denominator df = 102. Bold p-values denote $p < 0.05$; *italic* denotes $0.05 \le p < 0.10$.

Effect	$F(1102)$	p-value	Interpretation
Wood species	22.57	$\mathbf{6.7 \times 10^{-6}}$	Birch > Beech (overall)
Moisture content (MC)	35.63	$\mathbf{3.5 \times 10^{-8}}$	Wet ≪ Dry (large penalty)
Temperature	3.40	*0.068*	Cooling to −20°C: borderline gain
$\log_{10}$(loading rate)	8.14	**0.0053**	Faster loading ↑ f_m
Species × Temperature	8.72	**0.0039**	Temperature effect differs by species
Species × MC	9.15	**0.0031**	MC penalty differs by species
Temperature × MC	37.17	$\mathbf{2.0 \times 10^{-8}}$	Cooling helps mainly when dry
Species × Temperature × MC	9.52	**0.0026**	Significant three-way effect

Non-significant rate-interaction terms (all $p > 0.10$): Species × Rate, Temp × Rate, MC × Rate, Species × Temp × Rate, Species × MC × Rate, Temp × MC × Rate, and the four-way interaction.

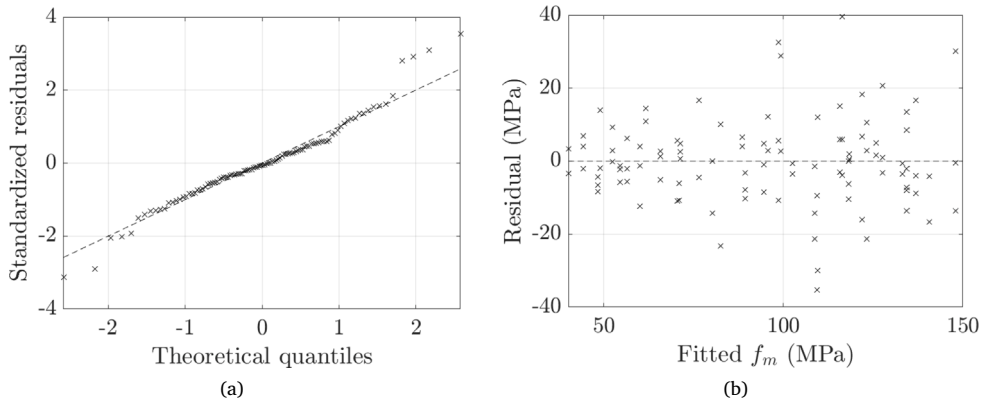

Fig. 9. Diagnostic checks for the linear mixed-effects model. (a) Normal Q–Q plot of standardized residuals; (b) Residuals versus fitted values.

when specimens are soaked. The main effect of temperature does not cross the 5% threshold ($p = 0.068$); however, its interactions remain relevant. The significant Species×Temperature term ($F = 8.7$) indicates that Birch benefits more from cooling than Beech, while the strong Temperature×MC interaction ($F = 37.2$) shows that −20 °C increases strength essentially only in dry specimens. The loading rate enters as a quantitative covariate; its main effect ($F = 8.1$, $p = 0.005$) corresponds to an average slope of about +7.8 MPa per decade in rate ($\log_{10}$). Importantly, none of the rate-interaction terms are significant ($p > 0.40$), implying that the rate slope is invariant with respect to species, moisture, and temperature. This simplifies design: once MC and T are fixed, the same rate amplification factor can be applied to both hardwoods.

Finally, the three-way interaction Species×Temperature×MC remains significant ($F = 9.5$, $p = 0.0026$), consistent with the empirical observation that Birch gains most when both dry and cold, whereas Beech shows only modest gains under the same conditions. No four-way interaction is significant, indicating that the model is not over-parameterized. From an engineering perspective, maintaining dowels dry yields the most substantial benefit; choosing Birch over Beech provides a secondary margin, and operating at −20 °C confers an additional margin only when moisture is adequately controlled.

The diagnostic plots in Fig. 9 confirm that the LME model satisfies the core assumptions required for valid inference. In the normal Q–Q plot (Fig. 9(a)), the standardized residuals align closely with the 45° reference, deviating only at the extreme upper tail. Such a minor departure, amounting to three points beyond the theoretical 97.5-percentile, is common in mechanical-test data and falls well within the robustness range of mixed models. The near-perfect linearity through the bulk of the distribution supports the use of t- and F-based tests reported in Table 7.

The residual-versus-fitted scatter (Fig. 9(b)) shows no funnel-shaped pattern or curvature: residuals remain homoscedastic across the fitted range (40–160 MPa) and cluster symmetrically around zero. A handful of large-positive points correspond to the highest-strength Birch–Dry specimens tested at the fastest rate; Cook's distances for these observations are below 0.3 (not shown), indicating they are not unduly influential. The diagnostics prove that the random-intercept structure adequately captures between-specimen variability, and the fixed-effect estimates and p-values can be interpreted without reservation.

Birch is significantly stronger than Beech (+22.3 MPa; $p < 10^{-5}$). The main temperature contrast (−20 °C vs. 20 °C) is positive but not significant at 5% ($p = 0.068$). Loading rate has a significant, modest slope of about +7.8 MPa per decade in $\log_{10}$ rate. Moisture content is the dominant driver: each additional 10 percentage points above the dry baseline reduces bending strength by ≈ 28.5 MPa (−24.8%; $p = 1.86 \times 10^{-16}$). In line with the ANOVA, rate-interaction terms are non-significant, so once MC and T are fixed the same rate amplification can be applied across species.

3.4. Discussion

Concerning temperature and moisture, a substantial body of work has examined clear wood from multiple species (Gerhards, 1982; Jiang et al., 2014; Zhao et al., 2016; Özkan, 2021; Ayrilmis et al., 2010a; Zhao et al., 2015; Szmutku et al., 2013). In general, decreasing temperature below freezing increases bending strength and stiffness due to reduced molecular mobility within the wood structure (Gerhards, 1982); for example, Gerhards reported strength increases between 50 °C and −50 °C of about 60% at moisture content (MC) 18%–20% and 11% at near-zero MC (Gerhards, 1982). More recent studies corroborate this trend: Özkan (Özkan, 2022) observed higher bending strength for frozen *Fagus orientalis* (12% MC) at cryogenic temperature compared to 20 °C, while Zhao et al. (2016) reported pronounced gains for *Betula platyphylla* that were strongest in water-saturated samples. Similar temperature-driven increases have been reported for wood-based panels, plywood, and chipboards (Ayrilmis et al., 2010a; Bekhta and Marutzky, 2007), often attributed to water freezing within the cell wall and the resulting stiffening/adhesion effects.

Beyond single freezing, cyclic exposure may be detrimental. Although Zhao et al. (2015) found limited changes in modulus of elasticity (MOE) after repeated freeze–thaw cycles for birch, other studies indicate that repeated cycles can reduce strength, stiffness, and deformation capacity (Asare et al., 2024; Hasan et al., 2004; Ayrilmis et al., 2010b; He et al., 2020), and severe degradation has been reported for engineered wood products after many cycles (Gao et al., 2024). Related work on thermal treatment at elevated temperatures shows improved dimensional stability and durability (Roszyk et al., 2020; Srinivas and Pandey, 2012), but often at the cost of reduced mechanical performance (He et al., 2021; Kloiber et al., 2010; Martinka et al., 2013; Moya et al., 2017).

Regarding loading rate, deformation speed can markedly influence bending strength because higher rates reduce the time available for viscoelastic deformation, typically leading to increased apparent strength and stiffness and, under impact-type scenarios, larger dynamic amplification (Cao et al., 2024).

Within this broader context, the trends observed for hardwood dowels in the present study are consistent with clear-wood evidence in that (i) moisture is the dominant driver of strength reduction due to plasticization of the lignocellulosic matrix, and (ii) sub-zero temperature can partially counteract this effect by increasing matrix stiffness once water is frozen. However, the magnitude of the temperature benefit measured here is modest (only a few percent) and becomes noticeable primarily at high moisture content, which is in line with the moisture-dependent freezing effects reported for clear wood (Gerhards, 1982; Zhao et al., 2016). In contrast, for dry-conditioned dowels the temperature effect is limited, suggesting that the dowel response is

governed more by the intrinsic dry-state stiffness than by temperature-induced changes. Concerning rate effects, the present results support the general viscoelastic argument (Cao et al., 2024) but indicate that, within the investigated quasi-static range, rate sensitivity is mainly relevant for dry (stiffer) dowels and becomes negligible after soaking, where moisture-induced softening dominates the response. Overall, these findings extend clear-wood observations to structural dowel elements and provide quantitative evidence for practical modification factors that account for coupled temperature–moisture conditions and the (limited) rate sensitivity relevant to dowel-based connection design.

4. Simplified design model for strength modification factor

Given the appreciable scatter in bending strength (a typical situation in timber engineering) and the practical need for simple, easy–to–apply models, the authors propose a factorized formulation to predict the bending strength under combined changes of temperature T, moisture content MC, and loading rate v. The model is deliberately elementary, yet it captures the dominant trends observed in the tests.

$$f_{m,\mathrm{d}}(T, MC, v, s) = \frac{f_{m,\mathrm{ref}}(s)\, \gamma_L(v)\, \gamma_{TM}(T, MC, s)}{\gamma_M}, \tag{2}$$

where $f_{m,\mathrm{d}}$ is the design bending strength (MPa), $f_{m,\mathrm{ref}}(s)$ the reference bending strength for species s (MPa), $\gamma_L(v)$ the loading–rate modification factor (Eq. (3)) and $\gamma_{TM}(T, MC, s)$ the combined temperature-moisture factor (species-dependent, Eq. (4)), while $s \in \{\mathrm{Beech}, \mathrm{Birch}\}$ denotes the species. The reference strengths used are

$$f_{m,\mathrm{ref}}(\mathrm{Beech}) = 115\ \mathrm{MPa}, \qquad f_{m,\mathrm{ref}}(\mathrm{Birch}) = 101\ \mathrm{MPa},$$

obtained from the dry, 20 °C, quasi-static condition ($v \le 1$ mm/min).

Inspection of the data and the statistical analysis suggest that a two–level rate factor is sufficient (a transition occurs around $v = 1$ mm/min):

$$\gamma_L(v) = \begin{cases} 1.00, & v \le 1\ \mathrm{mm\,min^{-1}}, \\ 1.30, & v > 1\ \mathrm{mm\,min^{-1}}. \end{cases} \tag{3}$$

Differences between species emerge mainly in the penalty associated with high moisture; a modest temperature effect is only apparent in wet conditions. No reduction is applied for dry specimens ($MC < 15\%$) at either 20 °C or −20 °C. For wet specimens ($MC \ge 15\%$), the following simplified model is proposed:

$$\gamma_{TM}(T, MC, s) = \begin{cases} 1.00, & MC < 15\%,\ T \in \{-20\ ^\circ\mathrm{C},\ 20\ ^\circ\mathrm{C}\}, \\ 0.40\ (\mathrm{Beech})\ /\ 0.50\ (\mathrm{Birch}), & MC \ge 15\%,\ T = 20\ ^\circ\mathrm{C}, \\ 0.60\ (\mathrm{Beech})\ /\ 0.70\ (\mathrm{Birch}), & MC \ge 15\%,\ T = -20\ ^\circ\mathrm{C}. \end{cases} \tag{4}$$

To achieve a 95% reliability that the measured strength exceeds the design value, a global material factor γ_M is calibrated empirically:

$$\gamma_M = Q_{0.95}\left(\frac{f_{m,\mathrm{pred}}}{f_{m,\mathrm{meas}}}\right), \tag{5}$$

where $Q_{0.95}(\cdot)$ denotes the 95th percentile, $f_{m,\mathrm{pred}}$ is the value from (2) without γ_M, and $f_{m,\mathrm{meas}}$ is the experimental strength. In other words, γ_M is chosen so that at least 95% of the measured values lie above $f_{m,\mathrm{d}}$.

The proposed model is intentionally simple, derived from direct inspection of the experimental ratios and guided by statistical trends, to balance accuracy with the ease of application in design practice. Fig. 10 compares the experimentally measured bending strengths with the values predicted by the proposed model. The associated error metrics are summarized in Table 8. Overall, the model exhibits a modest scatter (RMSE ≈ 18 MPa, MAE ≈ 14 MPa) and negligible bias (MBE ≈ 0.5 MPa), with $R^2 = 0.821$. This level of accuracy is acceptable for a simple, design-oriented formulation.

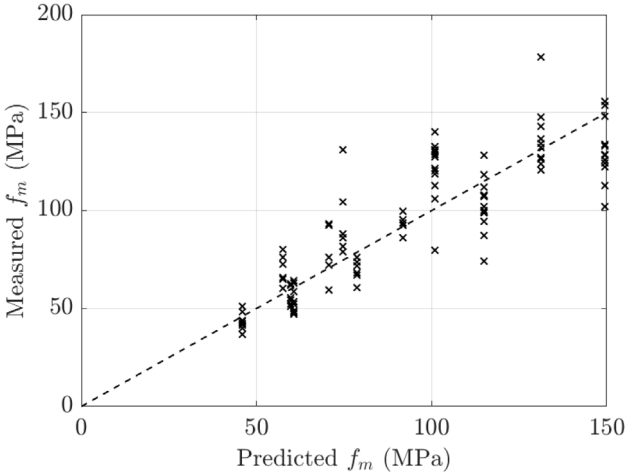

Fig. 10. Experimental vs. predicted bending strength values.

Table 8
Error metrics for the predictive model. RMSE = root-mean-square error; MAE = mean absolute error; MBE = mean bias error; R^2 = coefficient of determination.

Metric	RMSE (MPa)	MAE (MPa)	MBE (MPa)	R^2
Value	17.68	13.53	0.47	0.821

To ensure that 95% of the measured strengths exceed the design value, a partial safety factor γ_M was calibrated empirically from the ratio $f_{m,\mathrm{pred}}/f_{m,\mathrm{meas}}$. Species-specific values were obtained as:

$$\gamma_M(s) = \begin{cases} 1.327, & s = \mathrm{Beech}, \\ 1.269, & s = \mathrm{Birch}, \end{cases} \tag{6}$$

so a common value $\gamma_M = 1.30$ may be adopted for design. This γ_M is different from load-duration modifiers (e.g., Madison curve or k_{mod} in EN 1995-1-1), which act on mean strength. Current codes are not uniform on dynamic effects (e.g., $k_{\mathrm{mod}} \approx 1.10$ for instantaneous loads in EN 1995-1-1; CSA S850 allows 1.1-1.4), and blast studies often report dynamic increases ∼1.1 (Cao et al., 2024).

In the Eurocode 5 proposal, the dowel bending capacity is introduced via a characteristic bending moment and checked in conjunction with geometric and material prerequisites. The code maintains a generic formulation and delegates basic material properties to EN 338, while design safety is handled through the standard partial factor $\gamma_M = 1.3$ for timber and connections. The present work preserves the Eurocode's factorized spirit but introduces two modifiers, γ_L for rate and γ_{TM} for the joint temperature-moisture effect, directly calibrated on the experimental dataset. The model provides multipliers that engineers can apply without abandoning the established semi-probabilistic framework.

Additionally, the safety factor γ_M values (approximately 1.27–1.33 for the two species) are reassuringly close to the Eurocode recommendation 1.3, supporting the view that the proposed modifiers can be incorporated into current design practice without altering the overall level of safety.

It is worth noting that in design contexts, characteristic (5th percentile) strengths should be used; γ_M here is an empirically calibrated material factor consistent with EC5 magnitude and does not replace EC5's load-duration/impact provisions. $\gamma_L = 1.30$ is a dataset-specific quasi-static modifier, not an impact factor.

5. Assessment of the microstructure using SEM

To analyse the microscopic differences in failure modes and qualitatively correlate them with the previously described mechanical test

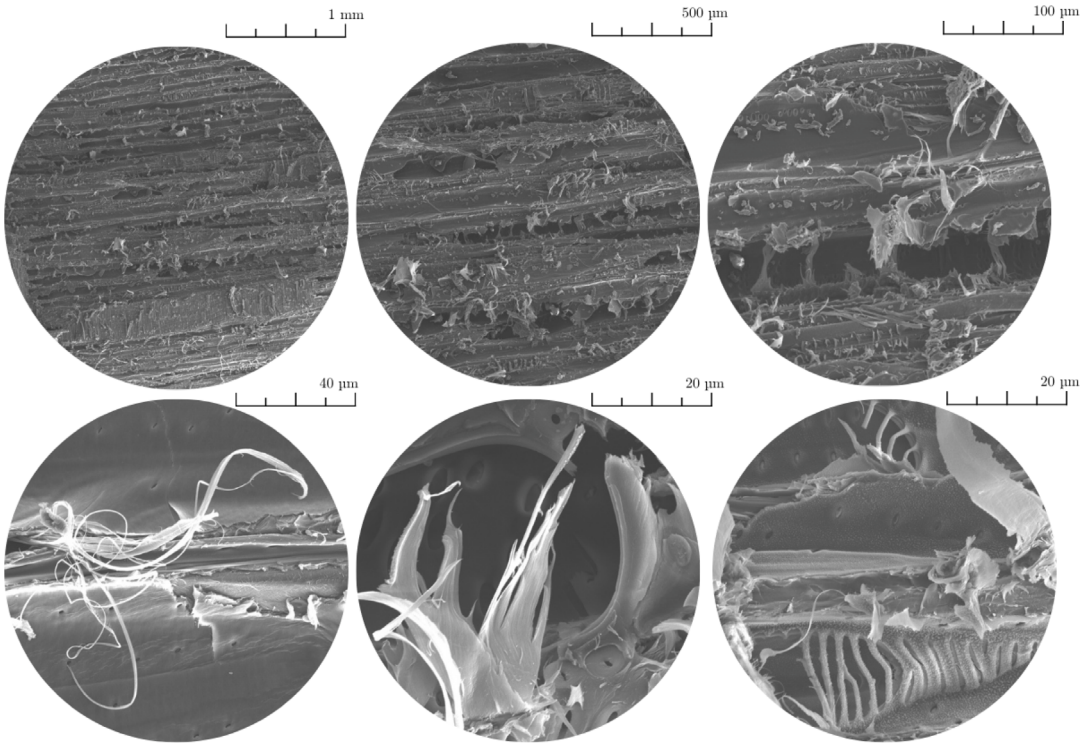

Fig. 11. Representative SEM micrographs of a Beech dowel fracture surface (Dry 20 °C) after bending. Images are arranged from left to right and top to bottom in increasing magnification, with the corresponding scale bars indicated above each frame.

results, SEM investigations were conducted in this study. Since the effects of loading rate, temperature, and moisture content are qualitatively similar in beech and birch, differing only in magnitude, the micrographic analysis was limited to beech specimens.

The microscopy observations were conducted using an SEM FEI Nova NanoSEM 450 at the CIGS laboratories of the University of Modena and Reggio Emilia. The specimens were placed in the SEM chamber with the treated fracture surface facing upward. The SEM operated in high-vacuum mode, utilizing a secondary electron detector. An accelerating voltage of 10 kV was applied to balance surface resolution and minimize charging effects, while the working distance was maintained between 5 and 7 mm to ensure optimal image sharpness.

The four specimens analysed with SEM correspond to the following conditions: Dry at 20 °C, Dry at −20 °C, Wet at 20 °C, and Wet at −20 °C. This selection allows for the investigation of microstructural differences in failure across all combinations of moisture content and temperature considered in this study. The obtained SEM micrographs are presented and discussed in the following sections.

The top row of micrographs in Fig. 11 displays images at magnifications of 100×, 200×, and 800×, from left to right. These images provide an overview of macroscopic fibre pull-out on the fracture surfaces. The bottom row presents high-magnification images, ranging from 3000× to 6000×, highlighting features such as cell-wall peeling, microfibrillar ribbons, and bordered-pit fracture.

The three upper micrographs (scale bars: 1 mm, 500 µm, and 100 µm) reveal a dominantly longitudinal failure mode: long fibres have been torn loose from the matrix, leaving elongated shear grooves and occasional "missing-fibre" trenches. In places, the compound middle lamella is still visible as a smooth, ribbon-like film adhering to the fracture plane, indicating that failure initiated by separation along the intercellular layer rather than by fibre rupture. Moving to higher magnification (lower row, 40 µm and 20 µm bars), the surface texture changes. Individual cell walls are delaminated and curled, exposing a network of micro-fibrillar ribbons that bridge the crack flanks. Some tracheids exhibit classic "trumpet" openings where bordered pits have been pulled apart, while others show brittle splintering of the secondary wall—evidence that radial cracks propagated through late wood bands of higher density. The isolated fibrils in the left-most bottom image testify to significant energy dissipation via fibrillation before final rupture. Taken together, the sequence demonstrates a multi-scale failure mechanism: (i) initial debonding along the middle lamella, (ii) fibre pull-out and inter-cellular shear, and (iii) progressive peeling and fibrillation of the secondary wall culminating in micro-pit rupture.

Fig. 12 presents SEM images of the beech dowels fractured under dry conditions but cooled to −20 °C. For ease of comparison, analogous magnifications used for the 20 °C reference (Fig. 11) are shown: 500 µm overview, 50 µm intermediate, and 40 µm sub-cellular. The frozen specimen exhibits a more facetted fracture surface with short radial offsets intersecting the longitudinal shear bands. In contrast, the room-temperature fracture displayed long, continuous pull-out grooves. The faceting is typical of a slightly more brittle response and is consistent with the modest (~5–10 MPa) increase in mean bending strength measured at −20 °C. At ambient temperature, abundant micro-fibrillar ribbons bridged the crack flanks. Under frozen conditions, the ribbons are markedly fewer and shorter; cell walls tend to detach cleanly after limited peeling. This reduction in micro-fibrillation indicates that the stiffer, colder matrix suppresses ductile tearing of the wall cells.

At the cell-wall level (20 µm), the −20 °C image shows sharper, angular ruptures of bordered-pit rims and secondary walls, whereas the 20 °C surface contains more plastically bent fibrils. No ice lenses or drying artifacts are visible, confirming that the moisture content remained below fibre saturation and that temperature alone accounts for the morphological shift. These observations confirm the statistical finding that temperature has, at best, a borderline main effect for beech ($p = 0.068$, Table 7). Cooling stiffens the ligno-cellulosic matrix, slightly reduces energy dissipation via micro-fibrillation, and thereby raises strength by ≈5–8%. The change is noteworthy yet small compared with the 47% strength loss caused by wetting.

Regarding the fracture morphology of wet beech at 20 °C, Fig. 13 shows the fracture surfaces with similar magnifications used for the

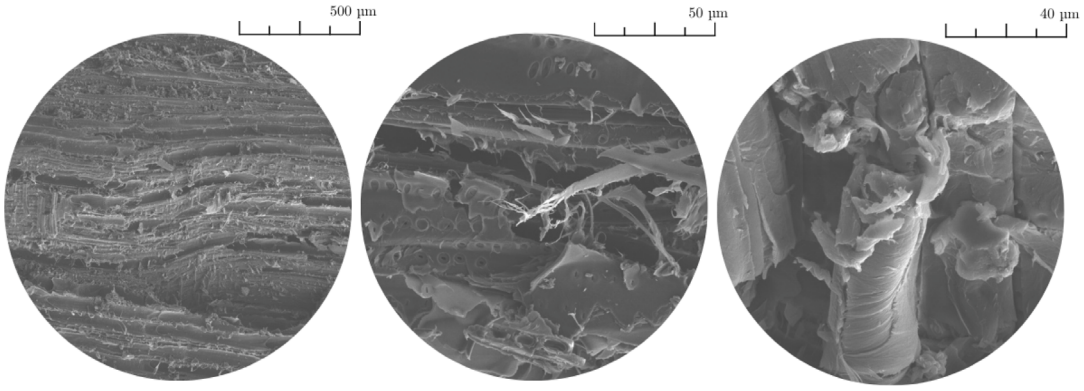

Fig. 12. Representative SEM micrographs of a Beech dowel (Dry −20 °C) fracture surface after bending. Images are arranged from left to right and top to bottom in increasing magnification, with the corresponding scale bars indicated above each frame.

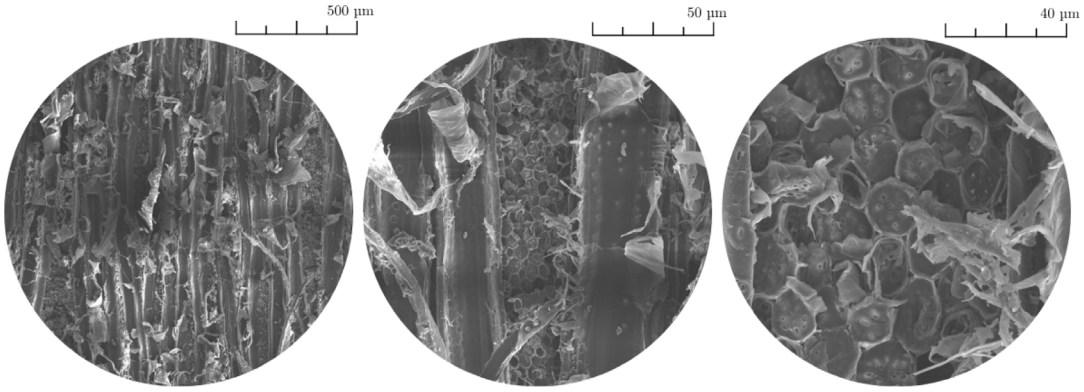

Fig. 13. Representative SEM micrographs of a Beech dowel (Wet 20 °C) fracture surface after bending. Images are arranged from left to right and top to bottom in increasing magnification, with the corresponding scale bars indicated above each frame.

dry specimens. At the macroscale morphology (500 µm), the fracture surface is rougher than its dry counterpart, with deep, ragged grooves and long fibre bundles protruding almost intact. Such extensive fibre pull-out indicates that the middle lamella yields in shear over large areas before any cell-wall rupture, a classic signature of moisture-softened hardwood. At the intermediate scale (100 µm), a honeycomb of unbroken early-wood lumina becomes evident, bordered laterally by plastically folded S_2 layers. These rounded folds are absent in the dry images and reflect the transition of the lignin matrix from a glassy to a rubbery behaviour once the moisture content exceeds the glass-transition threshold. Detached cell-wall sheets span several tracheids, confirming a peeling mechanism rather than brittle cleavage.

At higher magnification (right-side image), intact bordered pits and smooth cell corners dominate the field of view, demonstrating that crack propagation follows the lignin-rich middle lamella. Fractured secondary walls appear as flaky, ductile debris; angular splinters, so prominent in the frozen specimen, are almost absent. The high pit density also explains the rapid moisture equalization observed experimentally. The ductile morphology correlates with the 47% drop in mean bending strength for wet beech. Moisture reduces the cohesive strength of the middle lamella, allowing widespread fibre pull-out and thereby lowering the global stress required for crack advance.

The observed morphology arises from two moisture-driven mechanisms that operate simultaneously: (i) Plasticization of the middle lamella and (ii) Crack deflection and fibre twisting. Water molecules enter the lignin/hemicellulose matrix, lowering its glass-transition temperature and reducing its cohesive strength. The crack therefore prefers to propagate by shear along the weakened inter-cellular layer rather than through the cellulose walls, producing extensive fibre pull-out and ductile tearing. This accounts for the large roughness and the ≈ 47 % drop in mean strength recorded for wet beech. Once plasticized, not only the longitudinal middle lamella but also radial/tangential interfaces between fibre rows become weak. The advancing crack readily kinks into these planes, locally intersecting fibres in cross-section and exposing their nearly circular lumina—the honeycomb pattern seen at 100 µm and 40 µm magnification. In short, moisture transforms an essentially Mode I/II cleavage process (dry wood) into a highly tortuous, mixed-mode fracture in which crack deflection and fibre pull-out dominate energy dissipation.

Fig. 14 shows the fracture surface of wet beech at −20 °C. At the macroscale, the surface is dominated by long, largely intact fibre bundles; the deep honeycomb cavities typical of wet ambient fracture (Fig. 13) are absent. Freezing stiffens the lignin matrix and suppresses extensive crack deflection across the grain, so the crack remains mostly parallel to the fibres. Pull-out lengths are nevertheless longer than in dry wood, showing that the middle lamella is still weakened by the absorbed water.

Bundles of fibres separate cleanly, leaving clusters of irregular platelets wedged between them. These platelets are sheared fragments of the middle lamella and thin early-wood walls that have broken in a brittle manner rather than forming ductile ribbons. The morphology reflects the competing effects of temperature and moisture: ice stiffens the matrix (eliminating the ductile folds seen at 20 °C), yet the middle lamella remains the weakest link, so fibre pull-out persists. At the

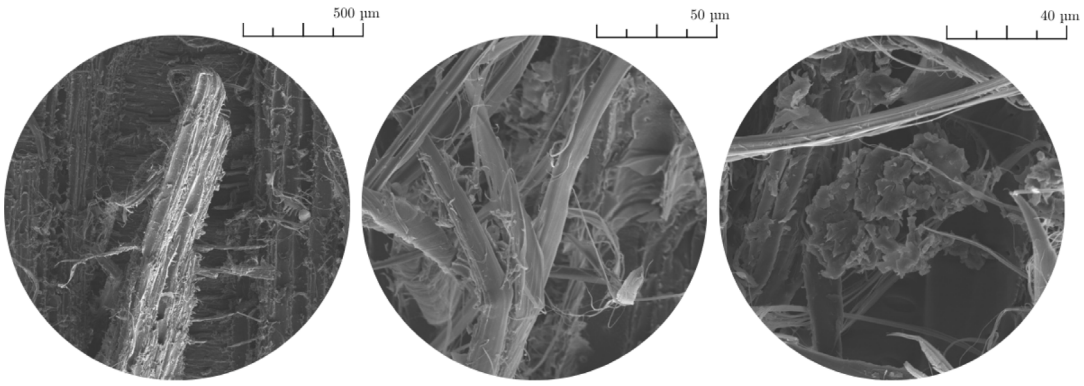

Fig. 14. Representative SEM micrographs of a Beech dowel (Wet -20 °C) fracture surface after bending. Images are arranged from left to right and top to bottom in increasing magnification, with the corresponding scale bars indicated above each frame.

highest magnification, the platelets appear as jagged flakes attached to smooth fibre surfaces. Unlike the room-temperature wet fracture, there is little evidence of fibrillar peeling; instead, the secondary wall fails by cleavage, leaving angular fragments. The absence of circular lumina confirms that the crack rarely deflects into the ray parenchyma when the matrix is frozen.

Therefore, freezing partially restores stiffness to the lignin network, leading to a cleaner, more brittle fracture and a modest increase in bending strength (+10–15 MPa relative to wet | 20 °C). However, because the middle lamella is still plasticized by its high water content, its cohesive strength remains lower than in dry wood, so fibre pull-out is not fully eliminated.

6. Conclusions

The present work investigated the bending strength of hardwood dowels, which are increasingly used in adhesive-free engineered timber products and all-wood structural joints. A laboratory campaign was carried out on beech and birch dowels (∅16 mm), testing two moisture states (dry and water-soaked; see Table 3), two temperatures (20 °C and −20 °C), and five quasi-static loading rates (v = 0.04, 0.2, 1, 5, 25 mm min^{-1}). The experimental outcomes were interpreted using a linear mixed-effects (LME) model and complemented by SEM observations of selected fracture surfaces.

With respect to the primary objective of quantifying the influence of environmental and loading conditions on dowel bending strength, moisture content emerged as the governing factor: water soaking reduced the mean bending strength by approximately 47 %. Species choice was the second most influential parameter, with birch exhibiting on average 19 % higher bending strength than beech. Cooling to −20 °C provided only modest strength gains (5 % to 8 %), and these gains were mainly observed in specimens with high moisture content. Within the investigated quasi-static range, loading-rate sensitivity was limited and became negligible once the dowels were water-soaked.

Regarding the objective of statistically separating main effects and interactions, the fitted LME model, including a random specimen intercept and $\log_{10} v$ as the rate descriptor, explained approximately 88% of the total variance and enabled inference for an unbalanced experimental design. The analysis highlighted a significant three-way interaction (Species×Temperature×Moisture), indicating that the temperature-related strength change depends on both species and moisture state. Diagnostic checks supported the adequacy of the model assumptions, with residuals reasonably close to normality and no evident heteroscedasticity trends.

Concerning the objective of linking macroscopic response to failure mechanisms, SEM observations were consistent with the statistical trends. Dry specimens exhibited predominantly brittle fracture features, whereas wet specimens tested at 20 °C showed more ductile behaviour characterized by fibre pull-out. Frozen-wet dowels displayed an intermediate morphology, suggesting that freezing partially restores matrix stiffness and reduces ductility relative to wet specimens at room temperature.

CRediT authorship contribution statement

Angelo Aloisio: Writing – review & editing, Writing – original draft, Visualization, Validation, Project administration, Methodology, Investigation, Formal analysis, Data curation, Conceptualization. **Yue Wang:** Writing – review & editing, Visualization, Validation, Investigation, Data curation. **Matteo Pelliciari:** Writing – review & editing, Data curation. **Yue Liu:** Writing – review & editing, Supervision. **Massimo Fragiacomo:** Writing – review & editing, Supervision.

Declaration of competing interest

The authors declare that they have no known competing financial interests or personal relationships that could have appeared to influence the work reported in this paper.

Acknowledgements

This work was supported by the Italian Ministry of University and Research (MUR) through the FIS3 research project "EXWOOD – Extending the Service Life of Engineered Wood and Bio-Based Materials under Multi-Hazards" (Grant No. FIS-2024-00457, CUP E53C25002310001), with Angelo Aloisio as the principal investigator.

The authors express their gratitude to Eng. Pasqualino Gualtieri for their valuable contributions to this research. Yue Wang greatly acknowledges the Lars Erik Lundberg Foundation (reference number: 1000891). Support by the University of Modena and Reggio Emilia, Italy through the project 'FAR Dipartimentale 2024–2025' (CUP E93C24000500005) is also acknowledged.

Appendix. Full results of the ANOVA test

See Table A.9.

Data availability

Data will be made available on request.

Table A.9
Type-III marginal F-tests from the linear mixed-effects model for bending strength f_m. The model includes all fixed-effect interactions among wood species, moisture content (MC), temperature, and $\log_{10}$ loading rate, with a random intercept for replicate (Specimen ID).

Effect	F	df_1	df_2	p	Interpretation[a]
Wood species	22.57	1	102	6.66e−06	Birch > Beech overall.
Moisture content (MC)	35.63	1	102	3.49e−08	Dry > Wet (large).
Temperature	3.40	1	102	6.81e−02	*Weak* benefit of −20 °C.
$\log_{10}$(Speed)	8.14	1	102	5.25e−03	Faster loading ↑ f_m.
Wood species × Temperature	8.72	1	102	3.92e−03	Temp effect differs by species.
Wood species × MC	9.15	1	102	3.15e−03	Moisture penalty differs by species.
Temperature × MC	37.17	1	102	1.95e−08	Cooling helps mainly when dry.
Wood species × $\log_{10}$(Speed)	0.03	1	102	8.67e−01	Rate effect similar across species.
Temperature × $\log_{10}$(Speed)	0.58	1	102	4.47e−01	No Temp × Rate interaction.
MC × $\log_{10}$(Speed)	0.48	1	102	4.88e−01	No MC × Rate interaction.
Wood species × Temperature × MC	9.52	1	102	2.62e−03	Triple interaction: context matters.
Wood species × Temperature × $\log_{10}$(Speed)	0.68	1	102	4.10e−01	n.s.
Wood species × MC × $\log_{10}$(Speed)	0.61	1	102	4.38e−01	n.s.
Temperature × MC × $\log_{10}$(Speed)	2.63	1	102	1.08e−01	trend only.
Wood species × Temperature × MC × $\log_{10}$(Speed)	1.64	1	102	2.03e−01	n.s.

[a] Direction inferred from model coefficients and descriptive means; adjust wording as needed.
Significance: **bold** $p < 0.05$; *italic* $0.05 \le p < 0.10$ (trend).

References

Aloisio, A., Pasca, D.P., Tomasi, R., Fragiacomo, M., 2025a. Sensitivity of bending stiffness to moisture content in adhesive-free wooden-doweled cross-laminated timber panels. Constr. Build. Mater. 490, 142143.

Aloisio, A., Wang, Y., Crocetti, R., Nyrud, A.Q., Tomasi, R., 2025b. Mechanical performance of pure-wood moment-resisting ridge joints with plywood gussets and wooden dowels. Eng. Struct. 334, 120271.

Aloisio, A., Wang, Y., Crocetti, R., Perstorper, M., Tomasi, R., Wålinder, M., 2026. Bending–shear domain of mode-V failure in hardwood dowels: Experimental tests and implications for dynamic grading. Eng. Struct. 349, 121882.

Asare, S., Stoescu, M., Balmori, L., Allena, S., Kidando, E., Owusu-Danquah, J., 2024. Freeze-thaw effect on the mechanical properties of different wood species: impact of moisture content variations, microscopic morphology, and thermal modification in a selected species. J. Infrastruct. Preserv. Resil. 5 (1), 1–19.

Ayrilmis, N., Buyuksari, U., As, N., 2010a. Bending strength and modulus of elasticity of wood-based panels at cold and moderate temperatures. Cold Reg. Sci. & Technol. 63 (1–2), 40–43. http://dx.doi.org/10.1016/j.coldregions.2010.05.004.

Ayrilmis, N., Buyuksari, U., As, N., 2010b. Bending strength and modulus of elasticity of wood-based panels at cold and moderate temperatures. Cold Reg. Sci. & Technol. 63 (1–2), 40–43. http://dx.doi.org/10.1016/j.coldregions.2010.05.004.

Beall, F.C., 2000. Subsurface sensing of properties and defects in wood and wood products. Subsurf. Sens. Technol. Appl. 1, 181–204.

Bekhta, P., Marutzky, R., 2007. Bending strength and modulus of elasticity of particleboards at various temperatures. Holz Als Roh - Werkst. 65 (2), 163–165. http://dx.doi.org/10.1007/s00107-006-0134-8.

Bohan, X., Shiyuan, J., Bilin, W., et al., 2022. Mechanical performance of timber-to-timber joints with densified wood dowels. J. Struct. Eng. 148 (04), 04022023. http://dx.doi.org/10.1061/(ASCE)ST.1943-541X.0003317.

Branco, J., Descamps, T., 2015. Analysis and strengthening of carpentry joints. Constr. Build. Mater. 97, 34–47. http://dx.doi.org/10.1016/j.conbuildmat.2015.05.089.

Cao, A.S., Houen, M., Frangi, A., 2024. Impact loading of glued laminated timber beams without finger-joints. Comput. Struct. 296, 107278.

Cave, I.D., 1968. The anisotropic elasticity of the plant cell wall. Wood Sci. Technol. 2, 268–278. http://dx.doi.org/10.1007/BF00352246.

Ceraldi, C., Lippiello, M., D'ambra, C., Prota, A., 2018. The influence of dowel-bearing strength in designing timber pegged timber joints. Int. J. Archit. Herit. 12 (3), 362–375.

Ceraldi, C., Lippiello, M., Russo Ermolli, E., 2012. Timber Pins Connect.: Reliab. Bolted Joints Des. Rules cited By 1.

Ceraldi, C., Mormone, V., Russo Ermolli, E., 2008. Restoring Timber Struct.: Connect. Timber Pegs cited By 1.

De Santis, Y., Aloisio, A., Fragiacomo, M., 2025. Stiffness prediction of wooden dowel connections with beam-on-foundation models. J. Struct. Eng. 151 (12), 04025220.

Derikvand, M., Khoshroodi, D.B., 2025. Experimental and analytical evaluation of shear capacity of reclaimed timber connections with thermo-mechanically densified wooden dowels. Constr. Build. Mater. 504, 144613.

Donaldson, L.A., 2008. Microfibril angle: measurement, variation and relationships—A review. IAWA J. 29 (4), 345–386. http://dx.doi.org/10.1163/22941932-90000210.

EN-408, 2003. BSi.

Field, A.P., Miles, J., 2012. Discovering Statistics Using R. Sage, London, Ch. 15: Checking model assumptions.

Frontini, F., Siem, J., lmo, R.R., 2020. Load-carrying capacity and stiffness of softwood wooden dowel connections. Int. J. Arch. Herit. 14 (03), 376–397. http://dx.doi.org/10.1080/15583058.2018.1547798.

Gao, S., Zhou, L., Xu, M., 2024. Freeze-thaw effect on performance degradation of recycled glulam from structural members after cyclic loading. J. Build. Eng. 88, http://dx.doi.org/10.1016/j.jobe.2024.109203.

Gerhards, C.C., 1982. Effect of moisture content and temperature on the mechanical properties of wood: an analysis of immediate effects. Wood Fiber Sci. 4–36.

Golovin, Y.I., Gusev, A.A., Golovin, D.Y., Matveev, S.M., Vasyukova, I.A., 2022. Multiscale mechanical performance of wood: from nano-to macro-scale across structure hierarchy and size effects. Nanomaterials 12 (7), 1139.

Grönquist, P., Schnider, T., Thoma, A., Gramazio, F., Kohler, M., Burgert, I., Rüggeberg, M., 2019. Investigations on densified beech wood for application as a swelling dowel in timber joints. Holzforschung 73, 559–568. http://dx.doi.org/10.1515/hf-2018-0106.

Haftkhani, A.R., Abdoli, F., Rashidijouybari, I., Garcia, R.A., 2022. Prediction of water absorption and swelling of thermally modified fir wood by artificial neural network models. Eur. J. Wood Wood Prod. 80 (5), 1135–1150.

Han, L., Kutnar, A., Sandak, J., Šušteršič, I., Sandberg, D., 2023. Adhesive-and metal-free assembly techniques for prefabricated multi-layer engineered wood products: A review on wooden connectors. Forests 14 (2), 311. http://dx.doi.org/10.3390/f14020311.

Hasan, M., Okuyama, H., Sato, Y., Ueda, T., 2004. Stress-strain model of concrete damaged by freezing and thawing cycles. J. Adv. Concr. Technol. 2 (1), 89–99. http://dx.doi.org/10.3151/jact.2.89.

He, K., Chen, Y., Sun, J., 2021. Axial mechanical properties of small-diameter round timber short columns after exposure to elevated temperatures. Wood Res. 65 (6), 925–936. http://dx.doi.org/10.37763/WR.1336-4561/65.6.925936.

He, K., Chen, Y., Wang, J., 2020. Axial mechanical properties of timber columns subjected to freeze-thaw cycles. J. Renew. Mater. 8 (8), 969–992. http://dx.doi.org/10.32604/jrm.2020.09573.

Jiang, J., Lu, J., Zhou, Y., Zhao, Y., Zhao, L., 2014. Compression strength and modulus of elasticity parallel to the grain of oak wood at ultra-low and high temperatures. BioResources 9 (2), 3571–3579. http://dx.doi.org/10.15376/biores.9.2.3571-3579.

Judd, J., Fonseca, F., Walker, C., Thorley, P., 2012. Tensile strength of varied-angle mortise and tenon connections in timber frames. J. Struct. Eng. 138 (5), 636–644. http://dx.doi.org/10.1061/(ASCE)ST.1943-541X.0000468, cited By 20.

Jung, K., Kitamori, A., Komatsu, K., 2008. Evaluation on structural performance of compressed wood as shear dowel. Holzforchung 62 (04), 461–467. http://dx.doi.org/10.1515/HF.2008.073.

Kloiber, M., Frankl, J., Drdácký, M., Bryscejn, J., Tippner, J., Kučerová, I., 2010. Change of mechanical properties of norway spruce wood due to degradation caused by fire retardants. Wood Res. 55 (4), 23–38.

Kretschmann, D., 2010. Mechanical properties of wood. In: Wood handbook: wood as an engineering ma- terial: chapter 5. Centennial ed.. General technical report FPL ; GTR-190. Madison, 5.1-5.46, (190), WI: US Dept. of Agriculture, Forest Service, Forest Products Laboratory,.

Kuznetsova, A., Brockhoff, P.B., Christensen, R.H.B., 2017. Lmertest package: Tests in linear mixed effects models. J. Stat. Softw. 82 (13), 1–26. http://dx.doi.org/10.18637/jss.v082.i13.

Laboratory, F.P., 2010. Wood Handbook—Wood as an Engineering Material. General Technical Report FPLGTR190, U.S. Department of Agriculture, Forest Service, Madison, WI, Tables on ray percentage, density and mechanical data.

Luke, S.G., 2017. Evaluating significance in linear mixed-effects models in r. Behav. Res. Methods 49, 1494–1502. http://dx.doi.org/10.3758/s13428-016-0809-y.

MacKay, R.B., 1997. Timber Frame Tension Joinery. University of Wyoming.

Martinka, J., Chrebet, T., Král, J., Balog, K., 2013. An examination of the behaviour of thermally treated spruce wood under fire conditions. Wood Res. 58 (4), 599–606.

Milch, J., Tippner, J., Brabec, M., Sebera, V., Kunecký, J., Kloiber, M., Hasníková, H., 2017. Experimental testing and theoretical prediction of traditional dowel-type connections in tension parallel to grain. Eng. Struct. 152, 180–187. http://dx.doi.org/10.1016/j.engstruct.2017.08.067, cited By 12.

Miller, J., 2004. Capacity of pegged mortise and tenon joinery. Capacit. Pegged Mortise Tenon Join..

Miller, J.F., Schmidt, R.J., Bulleit, W.M., 2010. New yield model for wood dowel connections. J. Struct. Eng. 136 (10), 1255–1261. http://dx.doi.org/10.1061/(ASCE)ST.1943-541X.0000224.

Moya, R., Fallas-Valverde, L., Berrocal, A., Méndez-Álvarez, D., 2017. Durability of thermally modified wood of gmelina arborea and tectona grandis tested under field and accelerated conditions. J. Renew. Mater. 5 (3–4), 208–219. http://dx.doi.org/10.7569/JRM.2017.634111.

Özkan, O., 2021. Effects of cryogenic temperature on some mechanical properties of beech (fagus orientalis lipsky) wood. Eur. J. Wood Wood Prod. 79 (2), 417–421. http://dx.doi.org/10.1007/s00107-020-01639-1.

Özkan, O.E., 2022. Effect of freezing temperature on impact bending strength and shore-d hardness of some wood species. BioResources 17 (4), 6123.

Panshin, A.J., de Zeeuw, C., 1980. Textbook of Wood Technology, fourth ed. McGraw–Hill, New York, Contains detailed vessel and ray dimensions for hardwoods.

Pinheiro, J.C., Bates, D.M., 2000. Mixed-Effects Models in S and S-PLUS. Springer, New York, ISBN 978-0-387-98957-0.

Pranata, Y., Kristianto, A., Darmawan, A., 2021. Elastic cross-section modulus ratio of Jabon (anthocephalus cadamba miq.) bolt-laminated timber beams. IOP Conf. Ser. Mater. Sci. Eng. 1071 (1), 012016. http://dx.doi.org/10.1088/1757-899X/1071/1/012016.

Riggio, M., Sandak, J., Sandak, A., 2016. Densified wooden nails for new timber assemblies and restoration works: A pilot research. Constr. Build. Mater. 102, 1084–1092. http://dx.doi.org/10.1016/j.conbuildmat.2015.06.045, cited By 33.

Roszyk, E., Stachowska, E., Majka, J., Mania, P., Broda, M., 2020. Moisture-dependent strength properties of thermally-modified fraxinus excelsior wood in compression. Materials 13 (7), 1–12. http://dx.doi.org/10.3390/ma13071647.

Sandberg, L., Bulleit, W., Reid, E., 2000. Strength and stiffness of oak pegs in traditional timber-frame joints. J. Struct. Eng. 126 (6), 717–723. http://dx.doi.org/10.1061/(ASCE)0733-9445(2000)126:6(717), cited By 65.

Satterthwaite, F.E., 1946. An approximate distribution of estimates of variance components. Biom. Bull. 2 (6), 110–114. http://dx.doi.org/10.2307/3002019.

Sotayo, A., Bradley, D.F., Bather, M., Oudjene, M., El-Houjeyri, I., Guan, Z., 2020. Development and structural behaviour of adhesive free laminated timber beams and cross laminated panels. Constr. Build. Mater. 259, 119821. http://dx.doi.org/10.1016/j.conbuildmat.2020.119821.

Srinivas, K., Pandey, K., 2012. Effect of heat treatment on color changes, dimensional stability, and mechanical properties of wood. J. Wood Chem. Technol. 32 (4), 304–316. http://dx.doi.org/10.1080/02773813.2012.674170.

Szmutku, M., Campean, M., Porojan, M., 2013. Strength reduction of spruce wood through slow freezing. Eur. J. Wood Wood Prod. 71 (2), 205–210. http://dx.doi.org/10.1007/s00107-013-0667-6.

Teodorescu, I., Pereira, B., Aquino, C., Branco, J., 2020. Experimental evaluation of dowel-type timber joints with wooden dowels. Proc. Inst. Civ. Eng.: Struct. Build. 173 (12), 927–938. http://dx.doi.org/10.1680/jstbu.20.00021, cited By 12.

Tomasi, R., De Santis, Y., Aloisio, A., Crocetti, R., Sæby, V.H., Nyrud, A.Q., 2025. Experimental and analytical investigation on timber connections with beech, birch and laminated densified wooden dowels. Constr. Build. Mater. 494, 142692.

Vilguts, A., Stamatopoulos, H., Malo, K.A., 2024. Experimental and analytical evaluation of semi-rigid timber connection with screwed-in threaded rods and steel coupling part. J. Build. Eng. 109923.

Wagenführ, R., 2006. Holzatlas, Sixth ed. Carl Hanser Verlag, Munich, Comprehensive atlas of wood anatomy and properties.

Wang, Y., Aloisio, A., Pasca, D.P., Tomasi, R., 2026. Buckling of adhesive-free wooden-dowelled cross-laminated timber panels. Eng. Struct. 348, 121806.

Wang, Y., Tomasi, R., Aloisio, A., Crocetti, R., Wang, T., 2025. Glued-in hardwood rods as reinforcements for compression perpendicular to the grain: Single fastener to global loading cases. Eng. Struct. 344, 121312.

West, B.T., Welch, K.B., Galecki, A.T., 2015. Linear mixed models: A practical guide using statistical software, second ed. CRC Press, Boca Raton, Ch. 2 : Random intercept models.

Xu, B.-H., Jiao, S.-Y., Wang, B.-L., Bouchaïr, A., 2022. Mechanical performance of timber-to-timber joints with densified wood dowels. J. Struct. Eng. 148 (4), 04022023. http://dx.doi.org/10.1061/(ASCE)ST.1943-541X.0003317.

Zhao, L., Jiang, J., Lu, J., 2016. Effect of thermal expansion at low temperature on mechanical properties of birch wood. Cold Reg. Sci. & Technol. 126, 61–65. http://dx.doi.org/10.1016/j.coldregions.2016.03.008.

Zhao, L., Lu, J., Zhou, Y., Jiang, J., 2015. Effect of low temperature cyclic treatments on modulus of elasticity of birch wood. BioResources 10 (2), 2318–2327. http://dx.doi.org/10.15376/biores.10.2.2318-2327.